Received: 13 May 2021 | Revised: 15 June 2021 | Accepted: 17 June 2021

DOI: 10.1111/cas.15036

ORIGINAL ARTICLE

Cancer Science WILEY

MUSASHI-2 confers resistance to third-generation EGFR-tyrosine kinase inhibitor osimertinib in lung adenocarcinoma

Reheman Yiming[1] | Yasuto Takeuchi[1] | Tatsunori Nishimura[1] | Mengjiao Li[1] | Yuming Wang[1] | Makiko Meguro-Horike[2] | Takashi Kohno[3] | Shin-ichi Horike[2] | Asuka Nakata[1] | Noriko Gotoh[1]

[1]Division of Cancer Cell Biology, Cancer Research Institute, Kanazawa University, Kanazawa City, Japan

[2]Division of Functional Genomics, Advanced Science Research Center, Kanazawa University, Kanazawa City, Japan

[3]Division of Genome Biology, National Cancer Center Research Institute, Tokyo, Japan

Correspondence
Noriko Gotoh, Division of Cancer Cell Biology, Cancer Research Institute, Kanazawa University, Kakuma-machi, Kanazawa City, Ishikawa 920-1192, Japan.
Email: ngotoh@staff.kanazawa-u.ac.jp

Funding information
Japan Agency for Medical Research and Development, Grant/Award Number: 16ck0106194h0001 and 16cm0106120h0001; Ministry of Education, Culture, Sports, Science and Technology, Grant/Award Number: 221S0002：JP17H06324; Japan Society for the Promotion of Science, Grant/Award Number: 17K19587 and 18H02679

Abstract

Epidermal growth factor receptor tyrosine kinase inhibitors (EGFR-TKIs) are effective in patients with non–small-cell lung cancer (NSCLC) harboring EGFR mutations. However, due to acquired resistance to EGFR-TKIs, even patients on third-generation osimertinib have a poor prognosis. Resistance mechanisms are still not fully understood. Here, we demonstrate that the increased expression of MUSASHI-2 (MSI2), an RNA-binding protein, is a novel mechanism for resistance to EGFR-TKIs. We found that after a long-term exposure to gefitinib, the first-generation EGFR-TKI lung cancer cells harboring the EGFR-TKI-sensitive mutations became resistant to both gefitinib and osimertinib. Although other mutations in *EGFR* were not found, expression levels of Nanog, a stemness core protein, and activities of aldehyde dehydrogenase (ALDH) were increased, suggesting that cancer stem-like properties were increased. Transcriptome analysis revealed that *MSI2* was among the stemness-related genes highly upregulated in EGFR-TKI-resistant cells. Knockdown of *MSI2* reduced cancer stem-like properties, including the expression levels of Nanog, a core stemness factor. We demonstrated that knockdown of *MSI2* restored sensitivity to osimertinib or gefitinib in EGFR-TKI-resistant cells to levels similar to those of parental cells in vitro. An RNA immunoprecipitation (RIP) assay revealed that antibodies against MSI2 were bound to *Nanog* mRNA, suggesting that MSI2 increases Nanog expression by binding to *Nanog* mRNA. Moreover, overexpression of MSI2 or Nanog conferred resistance to osimertinib or gefitinib in parental cells. Finally, *MSI2* knockdown greatly increased the sensitivity to osimertinib in vivo. Collectively, our findings provide proof of principle that targeting the MSI2-Nanog axis in combination with EGFR-TKIs would effectively prevent the emergence of acquired resistance.

KEYWORDS

cancer stem cells, gefitinib, gene expression profiling, non–small-cell lung cancer, RNA-binding protein

Reheman Yiming and Yasuto Takeuchi contributed equally to this work.

1 | INTRODUCTION

Lung cancer is the leading cause of cancer-related deaths worldwide.[1] Non–small cell lung cancer (NSCLC) is a major subtype of lung cancer, with adenocarcinoma being the most common subtype.[2] Lung adenocarcinoma is frequently associated with genetic changes in epidermal growth factor receptor (*EGFR*). Many patients with NSCLC harbor mutations in the tyrosine kinase domain of the *EGFR* (eg, exon 19 deletion and exon 21 L858R), resulting in the activation of EGFR, and they have benefited from treatment with EGFR-tyrosine kinase inhibitors (EGFR-TKIs).[3-5] However, in most cases, these patients eventually develop acquired resistance to EGFR-TKIs and are still associated with a poor prognosis.[6] The patterns of acquired resistance to first- and second-generation EGFR-TKIs largely overlap, and the gatekeeper point mutation in the tyrosine kinase domain of *EGFR*, *EGFR-T790M*, is the most common cause of acquired resistance.[7-9]

Osimertinib (AZD9291) is a third-generation irreversible oral EGFR-TKI that potently inhibits both EGFR-activating mutations and T790 M.[10-12] It shows less serious adverse events and high efficacy compared with the first- and second-generation EGFR-TKIs.[5] NSCLC patients with the EGFR-T790 M mutation[13,14] and even without the T790M mutation,[15] benefit from osimertinib treatment. However, similar to earlier generations of EGFR-TKIs, acquired resistance to osimertinib remains a major challenge. *EGFR*-resistant mutations (such as C797S and reversed to wild-type EGFR) occur in some relapsed patients. Other mechanisms of resistance include the activation of alternate receptor tyrosine kinases, such as HER2 overexpression and *MET* amplification; mutations in *PIK3CA*[16,17] and epithelial-mesenchymal transformation (EMT).[18] Many of these have also been reported as resistance mechanisms for first- and second-generation EGFR-TKIs.

Our group and others have reported that activation of the Wnt/β-catenin pathway is involved in primary and acquired resistance to gefitinib, a first-generation EGFR-TKI.[19,20] Although many efforts have been made to develop therapeutic strategies targeting the Wnt/β-catenin pathway,[21] there still remains no effective therapies without adverse effects, as the β-catenin pathway is essential for the functioning of a variety of normal cells, including stem cells. Novel targets that function specifically in cancer cells are urgently needed.

Recent emerging evidence has suggested that tumor tissues are composed of heterogeneous cell types, including a small population of cancer stem-like cells (CSCs) that appear to contribute to drug resistance and tumor recurrence. Therefore, targeted therapies against CSCs are important for overcoming drug resistance and preventing recurrence. Although several reports have shown that the acquisition of stem cell-like properties may be resistant to EGFR-TKIs,[22] how the stem-like properties are conferred remains obscure and there are no appropriate targets for CSCs in EGFR-TKI-resistant tumors.

The Musashi (MSI) family proteins are comprised of MSI1 and MSI2 in humans. In many normal tissues, they are expressed in overlapping patterns and function in a redundant manner.[23] Many studies have reported that either or both MSI proteins are overexpressed in a variety of tumor types and contribute to malignancy.[23,24] MSI proteins contain 2 N-terminal RNA recognition motifs (RRMs) that appear to regulate target gene expression by binding to the 3′ untranslated region of its mRNA.[25,26] The consequences of binding between MSI proteins and target mRNAs are complicated and appear to be cell context dependent. Recent reports have shown that MSI2 binding to the target mRNA may increase translation.[27]

In the present study, to identify novel targets to overcome resistance to EGFR-TKIs in lung adenocarcinoma, we focused on CSC properties. We analyzed gefitinib-resistant PC9M2 lung adenocarcinoma cells, which we previously established after long exposure to gefitinib, derived from PC9 cells that harbor exon 19 deletion mutations in *EGFR*. We compared the transcriptomes of aldehyde dehydrogenase (ALDH) activity-enriched CSC populations between PC9M2 and parental PC9 cells and found that MSI2 expression was markedly increased in PC9M2 cells. Our findings suggest that the increased expression of MSI2 confers not only CSC properties but also resistance to EGFR-TKIs in vitro and in vivo. MSI2 may interact with *Nanog* mRNA and increase stem-like properties and drug resistance. Targeting MSI2 in combination with EGFR-TKIs, such as osimertinib, may overcome drug resistance.

2 | MATERIALS AND METHODS

2.1 | Cell culture

PC9M2 cells were previously established as described.[19] H1975 and A549 cells were purchased from the ATCC. Cells were occasionally checked in mycoplasma-free conditions. All cells were cultured in RPMI-1640 medium (Nacalai Tesque) supplemented with 10% (v/v) fetal bovine serum (FBS) (Thermo Fisher Scientific), 100 units/mL penicillin, and 100 μg/mL streptomycin (Nacalai Tesque). HEK293T cells (Lenti-X 293T Cell Line) were purchased from Clontech and cultured in DMEM (Nacalai Tesque) supplemented with 10% (v/v) FBS (Thermo Fisher Scientific), 100 units/mL penicillin, and 100 μg/mL streptomycin (Nacalai Tesque). All cells used in these experiments were maintained in a humidified atmosphere of 5% CO_2 in air at 37°C.

2.2 | In vitro sensitivity analysis to gefitinib or osimertinib and cell proliferation assay

Cells (1-1.2 × 10^3) were plated onto a 96-well plate and treated with or without gefitinib (Cayman Chemical) or osimertinib (AZD 9291) (Selleck Chemicals). Control cells were treated with the same concentration of DMSO at the indicated concentrations. After 48 or 72 h of treatment, the cell viability was measured using the CellTiter 96® AQueous One Solution Cell Proliferation (MTS) Assay or

CellTiter-Glo® Luminescent Cell Viability Assay (Promega) following the manufacturer's protocol.

2.3 | ALDEFLUOR assay and flow cytometry

Aldehyde dehydrogenase (ALDH) activity was measured using an ALDEFLUOR Kit (STEMCELL Technologies), according to the manufacturer's protocol. Subsequently, cells were subjected to flow cytometric analysis using a FACSCanto II flow cytometer (BD Biosciences). Data were analyzed using FACS DIVA software (BD Biosciences), as previously described.[28]

2.4 | Immunoblotting

Cells were lysed in lysis buffer as described.[19] Western blotting was performed by standard procedures. Primary antibodies against MSI2 (#04-1069, Merck Millipore and #ab76148, Abcam), Nanog (#4903, Cell Signaling Technology), Sox2 (Cell Signaling Technology, #3579), and β-actin (MAB1501, Merck Millipore) were purchased. Horseradish peroxidase-conjugated secondary antibodies specific to mouse or rabbit IgG were used (GE Healthcare). Signals were detected using Immobilon (Merck Millipore).

2.5 | DNA microarray

Total RNA was extracted with RNeasy Mini Kit (Qiagen) according to the manufacturer's instructions. Cyanine-3 (Cy3) labeled cRNA was prepared from 0.2 μg RNA using the Low Input Quick Amp Labeling Kit (Agilent Technologies) according to the manufacturer's instructions. Dye incorporation and cRNA yield were checked with the NanoDrop ND-1000 spectrophotometer. Here, 0.6 μg of Cy3-labeled cRNA was hybridized to a SurePrint G3 Human GE microarray 8x60K Ver. 3.0 (G4858A #72363, Agilent Technologies) for 17 h at 65°C. After hybridization, slides were scanned immediately after washing on the Agilent DNA Microarray Scanner (G2539A) using the one color scan setting for 1 × 60K array slides (scan area 61 × 21.6 mm, scan resolution was 3 μm, the dye channel was set to Green and the Green photomultiplier tube (PMT) was set to 100%). The scanned images were analyzed using Feature Extraction Software 11.0.1.1 (Agilent) and default parameters (protocol AgilentG3_GX_1Color and Grid: 072363_D_F_20150612) to obtain background subtracted and spatially detrended Processed Signal intensities.

We determined that expression levels for each gene were significant when the absolute expression values of the genes were >1.5.

The raw data were deposited in the Gene Expression Omnibus (GEO) database, under number GSE168280.

Gene Ontology (GO) enrichment analysis (http://pantherdb.org/about.jsp) was performed using genes of which expression levels are >1.5-fold in the ALDH-positive (+) PC9M2 cell population compared with in the ALDH-positive (+) PC9 cell population.

2.6 | Sphere formation assay

Cells were trypsinized and washed in phosphate-buffered saline (PBS) (Thermo Fisher Scientific). A single cell suspension was plated into ultralow-attachment 96-well plates. DMEM/F-12 (Thermo Fisher Scientific) serum-free medium containing 20 ng/mL basic fibroblast growth factor (PeproTech), 20 ng/mL epidermal growth factor (Merck Millipore), B27 (Thermo Fisher Scientific), 4 μg/mL heparin (Stem Cell Technologies), 100 units/mL penicillin (Nacalai Tesque) and 100 μg/mL streptomycin (Nacalai Tesque) was used to cultivate the cells for 6 d as previously described.[29] The tumor spheres with a diameter >75 μm were counted under a light microscope.

2.7 | RNA immunoprecipitation (RIP) assay

RIP assay was carried out using a RIP assay Kit (Medical & Biological Laboratories) according to the manufacturer's instructions with minor modifications. Briefly, 1.5×10^7 PC9M2 cells were washed in ice-cold nuclease-free PBS and lysed with lysis buffer containing protease inhibitor, and 10 μL input samples were preserved for quality check (QC). In total, 60 μl of protein G sepharose beads (17061801, GE Healthcare) bound to 15 μg of Anti-MSI2 antibody (Ab 76148, abcam) or normal rabbit IgG (as a negative control) was incubated with cell lysate at 4°C for 3 h and washed with washing buffer containing dithiothreitol (DTT). Then 100 μL of the post-immunoprecipitation (IP) samples was preserved for QC by western blotting. RNAs were purified from the samples precipitated with antibodies or the post-IP samples (total RNA) and used for qPCR analysis.

2.8 | Statistical analysis

Statistics were computed using GraphPad Prism (version 8) software. For normally distributed datasets, significance was calculated using an unpaired, two-tailed Student *t* test. Data are presented as means ± SEM or means ± SD. The tumor growth datasets were analyzed using the Bonferroni-corrected two-way ANOVA to compute statistical significance. Data are presented as means ± SEM. Tumor-initiating cell frequency was analyzed by extreme limiting dilution analysis (ELDA) software (http://bioinf.wehi.edu.au/software/elda/), provided by the Walter and Eliza Hall Institute.[30] Quantification of immunoblotting results was performed using ImageJ software. Kaplan-Meier survival curves were analyzed by log-rank test. *P*-values: $P < .01$-.05 (*), $P < .001$-.01 (**), and $P < .0001$-.001 (***) were considered significant.

Detailed Materials and methods can be found in Document S1.

3 | RESULTS

3.1 | PC9M2 cells are resistant not only to gefitinib but also to osimertinib, and MSI2 is upregulated in PC9M2 cells

We previously established gefitinib-resistant PC9M2 cells derived from gefitinib-sensitive PC9 cells after culturing with gefitinib for several months.[19] PC9M2 cells harbor neither *EGFR* point mutations at T790M, HER2 upregulation, nor *MET* amplification.[19] We first examined the sensitivity of PC9M2 and parental PC9 cells to osimertinib. We treated cells with different doses of osimertinib or gefitinib for 72 h and analyzed the cell viability. We confirmed that PC9M2 cells were resistant to gefitinib compared with gefitinib-sensitive PC9 cells (Figure 1A). Although PC9 cells were sensitive to osimertinib as expected, we found that PC9M2 cells were significantly resistant to osimertinib (Figure 1B).

As we previously reported,[28] the expression levels of stemness genes *Nanog* and *Sox2* were greater in PC9M2 cells compared with in PC9 cells (Figure 1C). Western blotting revealed that the amount of Nanog protein was greater in PC9M2 cells compared with in PC9M2 cells (Figure 1D). The cell population with high ALDH activity, one of the CSC properties, was greater in PC9M2 cells compared with in PC9 cells (Figure 1E). These results confirmed that PC9M2 cells have more CSC properties.

We hypothesized that genes responsible for resistance to EGFR-TKIs would be more highly expressed in CSCs in PC9M2 cells than in PC9 cells. To identify novel targets to overcome osimertinib resistance based on CSC properties, we performed DNA microarray analysis and compared the transcriptomes of ALDH-positive cell populations between PC9 and PC9M2 cells. Gene set enrichment analysis (GSEA) revealed that 2 stemness-related gene sets were significantly upregulated in PC9M2 cells compared with PC9 cells (Figure 2A). GO analysis corroborated that progenitor or stemness-related genes were significantly upregulated in PC9M2 cells compared with PC9 cells (Figure 2B). In addition, the Wnt signaling pathway was upregulated as expected.[19] Nine genes overlapped in both gene sets derived from GSEA are indicated in the volcano plot (Figure 2C). Among the genes highly upregulated in PC9M2 cells compared with PC9 cells, the top gene was *TCF4* that

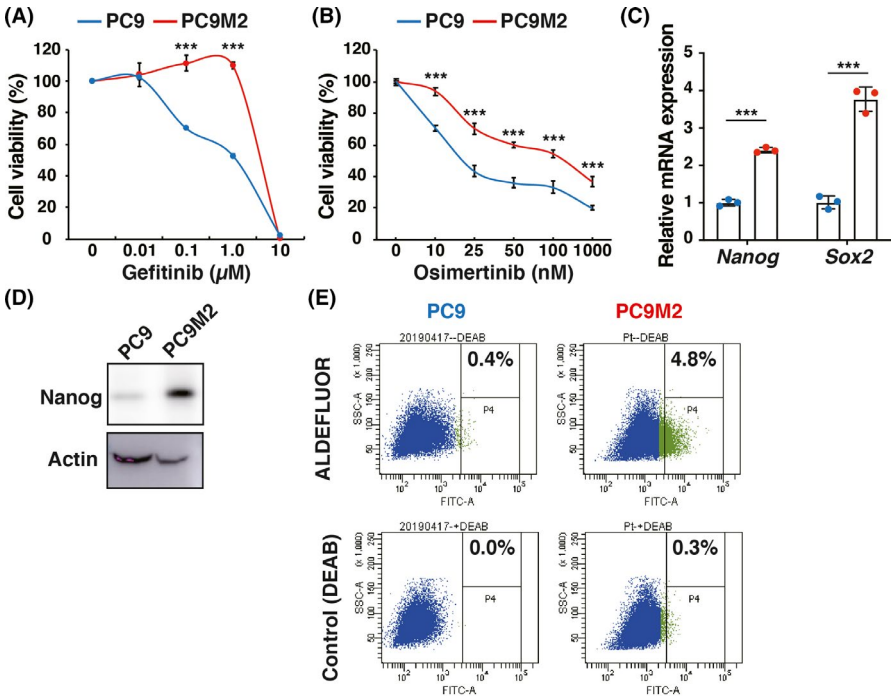

FIGURE 1 PC9M2 cells show resistance to gefitinib and osimertinib and an increase in CSC properties compared with PC9 cells. A and B, PC9 and PC9M2 cells were seeded in 96-well plates and treated with the indicated concentrations of gefitinib (A) and osimertinib (B) for 72 h, and cell viability was measured using MTS assay. Error bars indicate SD. A non-linear regression curve was generated using MTS data. n = 3 biologically independent experiments per treatment and experiments were repeated at least 3 times. C, *Nanog* and *Sox2* transcript levels were analyzed by real-time quantitative PCR (qPCR) in PC9 and PC9M2 cells relative to the expression of β-actin. Statistical significance was determined by unpaired, two-tailed Student *t* test. Results are shown as means ± SD. n = 3 biologically independent experiments and experiments were repeated at least 3 times. D, Immunoblotting analysis of Nanog expression in PC9 and PC9M2 cells. β-Actin was used as the loading control. Experiments were repeated at least 3 times and representative results were shown. E, ALDEFLUOR assay was performed using PC9 and PC9M2 cells. The aldehyde dehydrogenase (ALDH)-positive cell population was more enriched in PC9M2 cells than in PC9 cells (upper panels). Cells were pre-treated with the ALDH inhibitor, *N*,*N*-diethylaminobenzaldehyde (DEAB) (control, lower panels). The number (%) indicates the proportion of ALDH-positive cells. The data shown are representative of 3 independent experiments

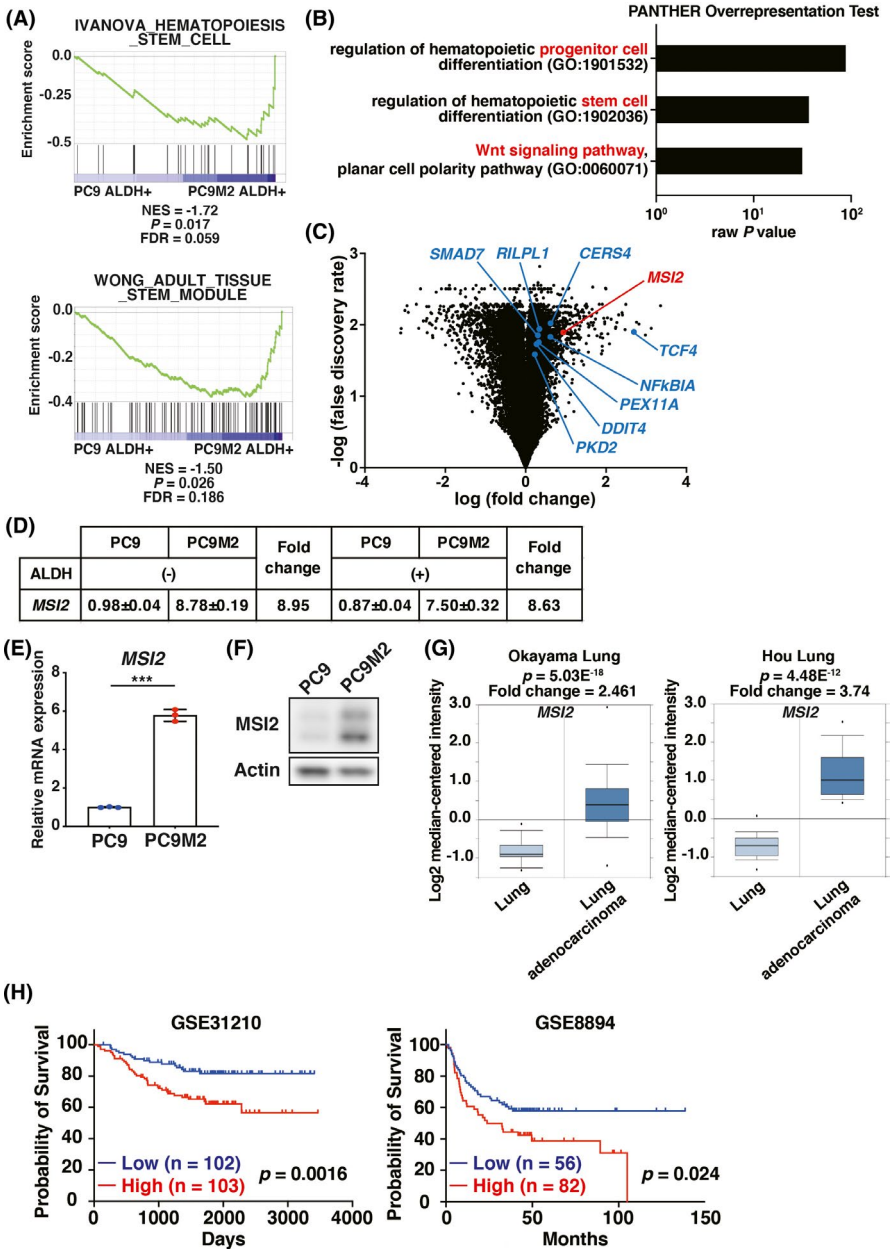

	PC9	PC9M2	Fold change	PC9	PC9M2	Fold change
ALDH	(-)			(+)		
MSI2	0.98±0.04	8.78±0.19	8.95	0.87±0.04	7.50±0.32	8.63

FIGURE 2 MSI2 expression is increased in PC9M2 cells compared with PC9 cells and lung adenocarcinoma patients with high expression of *MSI2* show poorer prognosis. A, Gene Set Enrichment Analysis (GSEA) results using genes of which expression levels are >1.5-fold in the ALDH-positive (+) PC9M2 cell population compared with in the ALDH-positive (+) PC9 cell population. Significantly enriched stem cell-related gene sets were shown: IVANOVA_HAEMATOPOIESIS_STEM_CELL (upper panel) and WONG_ADULT_TISSUE_STEM_MODULE (lower panel). FDR, false discovery rate; NES, normal enrichment score. B, Gene Ontology (GO) enrichment analysis was performed using genes of which expression levels are >1.5-fold in the ALDH-positive (+) PC9M2 cell population than in the ALDH-positive (+) PC9 cell population. C, Volcano plot of gene expression profiles. Fold changes of expression levels in ALDH-positive (+) PC9M2 cells with respect to those of ALDH-positive (+) PC9 cells. n = 3 biologically independent experiments per cell population. Overlapped 9 genes that include *MSI2* between both stem cell-related gene sets (A) are indicated in the plot. D, Mean expression values of *MSI2* in ALDH-negative (–) PC9 cells and ALDH-negative (–) PC9M2 cells and fold changes of expression levels in ALDH-negative (–) PC9M2 cells with respect to those of ALDH-negative (–) PC9 cells are shown (left half column). Mean expression values of MSI2 in ALDH-positive (+) PC9 cells and ALDH-positive (+) PC9M2 cells and fold changes of expression levels in ALDH-positive (+) PC9M2 cells with respect to those of ALDH-positive (+) PC9 cells were shown (right half column). E and F, *MSI2* expression in PC9 and PC9M2 cells was validated by qPCR (E) and immunoblotting (F). Statistical significance was determined by unpaired, two-tailed Student *t* test. Results are shown as means ± SD. n = 3 biologically independent experiments and experiments were repeated at least 3 times. G, *MSI2* expression was increased in lung adenocarcinoma tissues compared with normal lung tissues analyzed using the Oncomine database. H, Kaplan-Meier plots of overall survival according to *MSI2* gene expression level (high/low) that were split by the median value from 2 GEO datasets (GSE31210 and GSE8894)

encodes a core transcription factor downstream of Wnt/β-catenin pathway[31] (Table S1). We then focused on *MSI2*, as it is the second from the top. The expression levels of *MSI2* were 8.63-fold higher in ALDH-positive (+) cell populations in PC9M2 than those of PC9 cells (Figure 2D). We further analyzed the transcriptome in ALDH-negative (–) cell populations between PC9 and PC9M2 cells. We found that expression levels of *MSI2* were 8.95-fold higher even in ALDH-negative (–) cell populations in PC9M2 cells than those of ALDH-low PC9 cells (Figure 2D). These results suggested that *MSI2* is expressed at much higher levels in not only CSC populations, but also in ALDH-negative or non-CSC cell populations in PC9M2 cells than in PC9 cells. Quantitative polymerase chain reaction (qPCR) and western blotting confirmed that MSI2 was expressed at much higher levels in PC9M2 cells than in PC9 cells in bulk cell populations (Figure 2E,F). In contrast, another family member, *MSI1*, was expressed at very low levels in both PC9 cells and PC9M2 cells and there was little difference in expression levels between PC9M2 and PC9 cells (Figure S1A).

Oncomine analysis revealed that the expression levels of *MSI2* were higher in lung adenocarcinoma tissues than in normal tissues (Figure 2G). NSCLC patients with higher *MSI2* expression levels had a poorer prognosis in several cohorts of gene expression profiles. (Figure 2H).

3.2 | MSI2 depletion increases the sensitivity to gefitinib and osimertinib and decreases CSC properties in vitro

To examine whether MSI2 contributed to the efficacy of EGFR-TKIs, we depleted MSI2 in PC9M2 cells using shRNAs for *MSI2* using a lentivirus-based system. We found that MSI2 was efficiently depleted at the mRNA and protein levels using 2 types of shRNAs compared with control shRNA (Figure 3A,B). We found that cell growth was not significantly affected by *MSI2* depletion (Figure 3C). We then treated the cells with different doses of gefitinib or osimertinib. We found that depletion of *MSI2* in PC9M2 cells greatly increased sensitivity to both gefitinib and osimertinib up to levels similar to those of parental PC9 cells (Figure 3D-F).

Next, we examined CSC properties in these cells. We found that the depletion of *MSI2* decreased the expression levels of *Nanog* and *Sox2*, core stemness factors, at the mRNA level (Figure 4A). We confirmed that Nanog expression was decreased at the protein level following *MSI2* depletion (Figure 4B,C). Depletion of *MSI2* also decreased the activity of ALDH (Figure 4D). CSCs form spheroids in floating conditions in serum-free sphere culture medium (SCM), which contains a mixture of several growth factors and hormones. Tumor sphere-forming ability is another important property of CSCs. We cultured serially diluted cells in SCM. The tumor sphere-forming ability is determined as "tumor-initiating cell frequency" using ELDA.[30] We found that the frequency of tumor-initiating cells was greatly decreased in cells in which *MSI2* was depleted compared with control cells (Figure 4E-G).

To corroborate our findings, we used 2 other lung adenocarcinoma cell lines, H1975 and A549. H1975 cells harbor both the EGFR-TKI sensitive mutation *EGFR L858R* and acquired resistance mutation *EGFR T790M*. A431 cells harbor overexpression of EGFR and *KRAS* mutations and are EGFR-TKI resistant. Depletion of MSI2 using 2 types of shRNAs significantly increased the sensitivity to gefitinib and osimertinib (Figure S1B). Furthermore, the expression levels of *Nanog* and *Sox2* were decreased in cells in which *MSI2* was depleted compared with control cells in A549 cells (Figure S1C). We further analyzed the tumor sphere-forming ability of the A549 cells. We found that the tumor-initiating cell frequency was greatly decreased in cells in which MSI2 was depleted compared with control cells (Figure S1D).

Collectively, MSI2 appears to play an important role in gefitinib and osimertinib resistance and CSC properties.

3.3 | MSI2 binds to mRNA of *Nanog* and overexpression of MSI2 or Nanog confers resistance to gefitinib and osimertinib

We hypothesized that MSI2 may increase the expression of core stemness factors in cancer cells, leading to an increase in CSC properties and resistance to EGFR-TKIs. To test this hypothesis, we first searched for consensus binding sites for RRMs of MSI2 (UAG motifs or poly-U sequences) in stemness core factor genes.[23,32,33] We then found multiples of such sequences for MSI2 that were scattered over ~1 kb in the 3′ untranslated regions of *Nanog*. To examine whether MSI2 binds to *Nanog* mRNA, we performed a RIP assay. We incubated PC9M2 cell lysates with anti-MSI2 antibodies or control rabbit IgG. The immunoprecipitated samples were subjected to qPCR using primers designed to amplify *Nanog* mRNA. We found that anti-MSI2 antibodies precipitated MSI2 protein together with a significant amount of *Nanog* mRNA, while control rabbit IgG did not precipitate MSI2 protein or *Nanog* mRNA at detectable levels (Figure 5A,B). This finding suggests that MSI2 binds to *Nanog* mRNA in PC9M2 cells.

Next, we examined the effects of MSI2 overexpression in EGFR-TKI-sensitive PC9 cells. We transfected the expression vector encoding cDNA for *MSI2* into PC9 cells and obtained cells in which MSI2 was overexpressed (Figure 5C,D). We found that the expression levels of Nanog were increased at the protein level but not at the mRNA level (Figure 5C-E). We then treated the cells with different doses of gefitinib or osimertinib for 72 h. We found that PC9 cells overexpressing MSI2 were resistant to gefitinib or osimertinib compared with parental PC9 cells (Figure 5F,G).

We further examined the effects of Nanog overexpression in PC9 cells. We transfected the expression vector encoding cDNA for *Nanog* into PC9 cells and obtained cells in which *Nanog* was overexpressed (Figure 5H). We found that these cells were resistant to gefitinib or osimertinib compared with parental PC9 cells to some extent (Figure 5I,J).

Collectively, our findings indicated that overexpression of MSI2 or Nanog conferred resistance to EGFR-TKIs in PC9 cells.

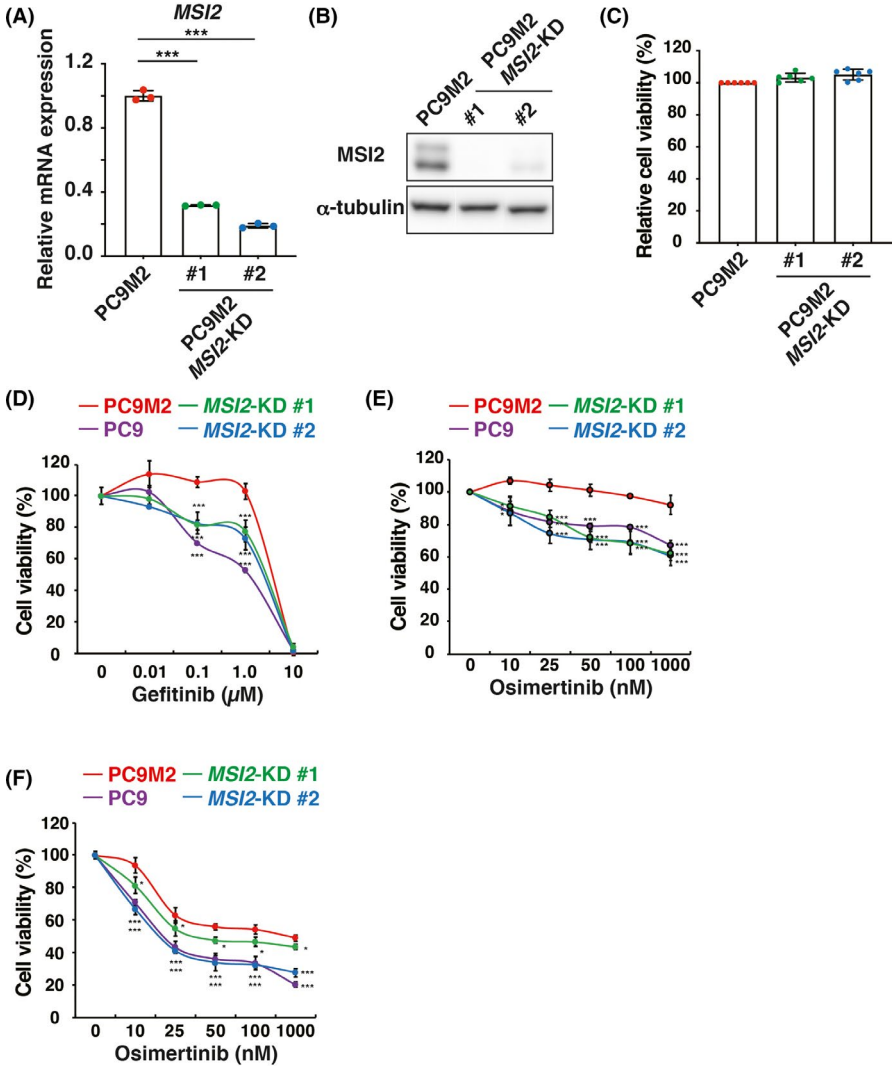

FIGURE 3 Depletion of *MSI2* restores gefitinib and osimertinib sensitivity of PC9M2 cells. A, PC9M2 cells were transduced with shRNAs for *MSI2* (*MSI2*-KD #1, *MSI2*-KD #2) or control shRNA (PC9M2). Knockdown efficiency using shRNAs for *MSI2* in PC9M2 cells was analyzed by qPCR. Statistical significance was determined by unpaired, two-tailed Student *t* test. Results are shown as means ± SD. n = 3 biologically independent experiments and experiments were repeated at least 3 times. B, Knockdown efficiency using shRNAs for *MSI2* in PC9M2 cells was analyzed by immunoblotting. α-tubulin was used as the loading control. Experiments were repeated at least 3 times and representative results were shown. C, Cells were seeded and cultured in the regular medium. After 72 h cell growth activity was analyzed by MTS assay. D-F, PC9M2 cells transduced with shRNAs for *MSI2* (*MSI2*-KD #1, *MSI2*-KD #2) or control shRNA (PC9M2) and parental PC9 cells were treated with the indicated concentrations of gefitinib (D) for 72 h, and osimertinib for 48 h (E) and 72 h (F). Cell viability was measured using MTS assay. Error bars indicate SD. A non-linear regression curve was generated using MTS data. n = 3 biologically independent experiments per treatment and experiments were repeated at least 3 times

3.4 | MSI2 depletion greatly increases the sensitivity to osimertinib in vivo

Finally, we examined the effects of MSI2 in vivo using a xenograft model. We first examined whether MSI2 contributed to tumorigenesis. We subcutaneously inoculated PC9M2 cells in which *MSI2* was depleted using shRNA for *MSI2* or control PC9M2 cells into the flanks of immunocompromised NSG mice and observed tumorigenesis. We found that tumor growth was not significantly affected by depletion of *MSI2*, and tumor weight and size were similar between *MSI2*-depleted cells and control cells (Figure 6A-C). This finding suggested that MSI2 is not strongly involved in tumor growth.

We then examined whether MSI2 contributed to osimertinib sensitivity. We inoculated PC9M2 cells in which *MSI2* was depleted using shRNA for *MSI2* or control PC9M2 cells into NSG mice and treated with osimertinib starting from the 7th day after inoculation. Tumor regression was clearly observed by the depletion of *MSI2* (Figure 6D-F). Our findings indicated that *MSI2* depletion greatly increased sensitivity to osimertinib in vivo. The combination of osimertinib and MSI2 inhibition is a promising strategy to prevent the emergence of acquired resistance.

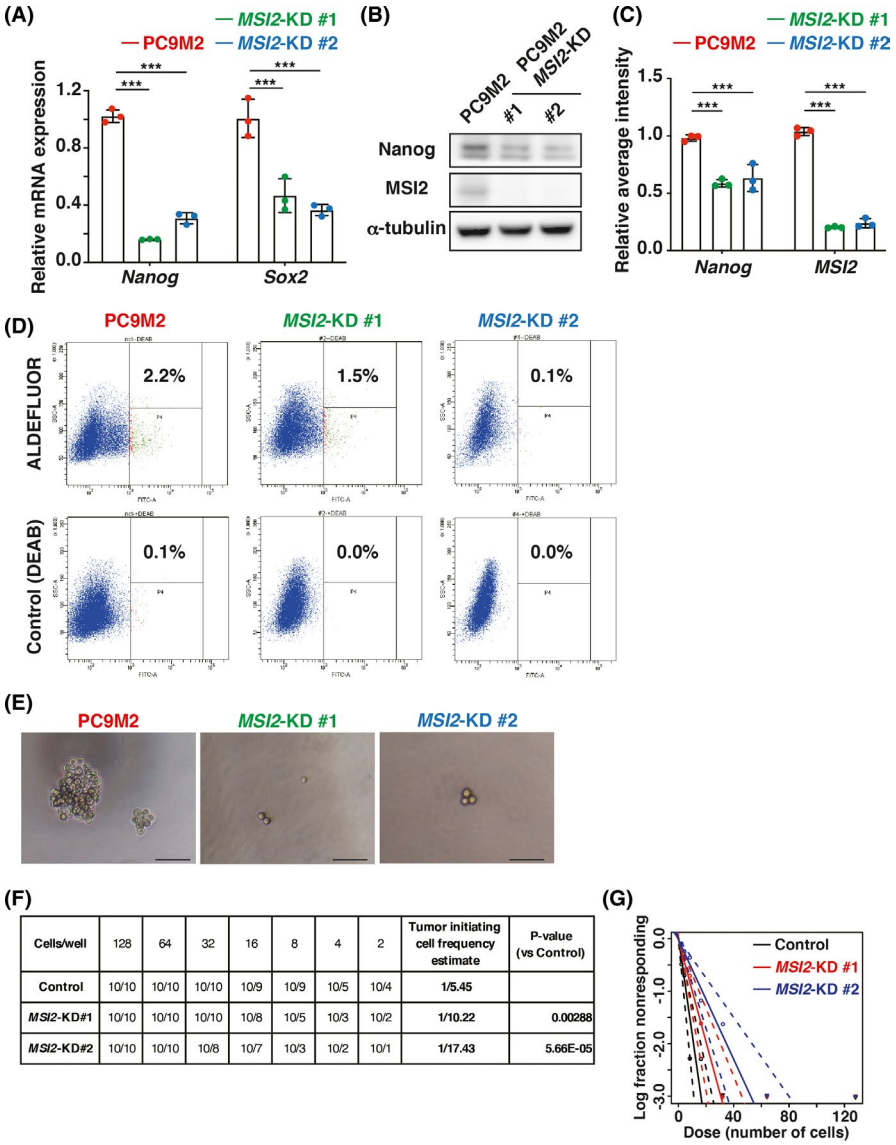

Cells/well	128	64	32	16	8	4	2	Tumor initiating cell frequency estimate	P-value (vs Control)
Control	10/10	10/10	10/10	10/9	10/9	10/5	10/4	1/5.45	
MSI2-KD#1	10/10	10/10	10/10	10/8	10/5	10/3	10/2	1/10.22	0.00288
MSI2-KD#2	10/10	10/10	10/8	10/7	10/3	10/2	10/1	1/17.43	5.66E-05

FIGURE 4 Depletion of MSI2 decreases the CSC properties in PC9M2 cells. A, Levels of *Nanog* and *Sox2* transcripts were analyzed by qPCR in PC9M2 cells transduced with shRNAs for *MSI2* (*MSI2*-KD #1, *MSI2*-KD #2) or control shRNA (PC9M2) relative to the expression of β-actin. Statistical significance was determined by unpaired, two-tailed Student *t* test. Results are shown as means ± SD. n = 3 biologically independent experiments and experiments were repeated at least 3 times. B, Immunoblotting analysis of MSI2 and Nanog expression in control and *MSI2* knockdown PC9M2 cells. α-tubulin was used as the loading control. Representative results were shown. C, Intensities of the immunoblotting bands in (B) were calculated using ImageJ software and normalized with those of α-tubulin. Statistical significance was determined by unpaired, two-tailed Student *t* test. Results are shown as means ± SD. n = 3 biologically independent experiments. D, The ALDH-positive cell population was decreased by *MSI2* knockdown in PC9M2 cells (upper panels). PC9M2 and *MSI2* knockdown cells were pre-treated with the ALDH inhibitor, DEAB (lower panels). The number (%) indicates the proportion of ALDH-positive cells. The data shown are representative of 3 independent experiments. E, Representative images of tumor spheroids derived from PC9M2 control (PC9M2) and *MSI2* knockdown (*MSI2*-KD #1, *MSI2*-KD #1) cells. Scale bar = 75 μm. F and G, In vitro limiting dilution assay for PC9M2 control (PC9M2) and *MSI2* knockdown (*MSI2*-KD #1, *MSI2*-KD #2) cells: 128, 64, 32, 16, 8, 4, and 2 cells/well were seeded in each well of a 96-well ultra-low attachment plate. Results were obtained 6 d after seeding (n = 10). CSC frequency and *P*-values were determined using the ELDA software (F). The amount of initially seeded cells (*x*-axis) is plotted against the log fraction of non-responders corresponding to wells without any detected spheres (*y*-axis). The slope of the line represents the log-active cell fraction (G)

4 | DISCUSSION

In this study, we demonstrated that increased expression of MSI2 is a novel mechanism for acquired resistance to EGFR-TKIs, including osimertinib. Increased expression of MSI2 may enhance the expression of Nanog, leading to an increase in CSC properties. Targeting MSI2 combined with EGFR-TKIs may overcome drug resistance and prevent recurrence.

We further showed that depletion of *MSI2* increased sensitivity to gefitinib or osimertinib in drug-resistant cells with or

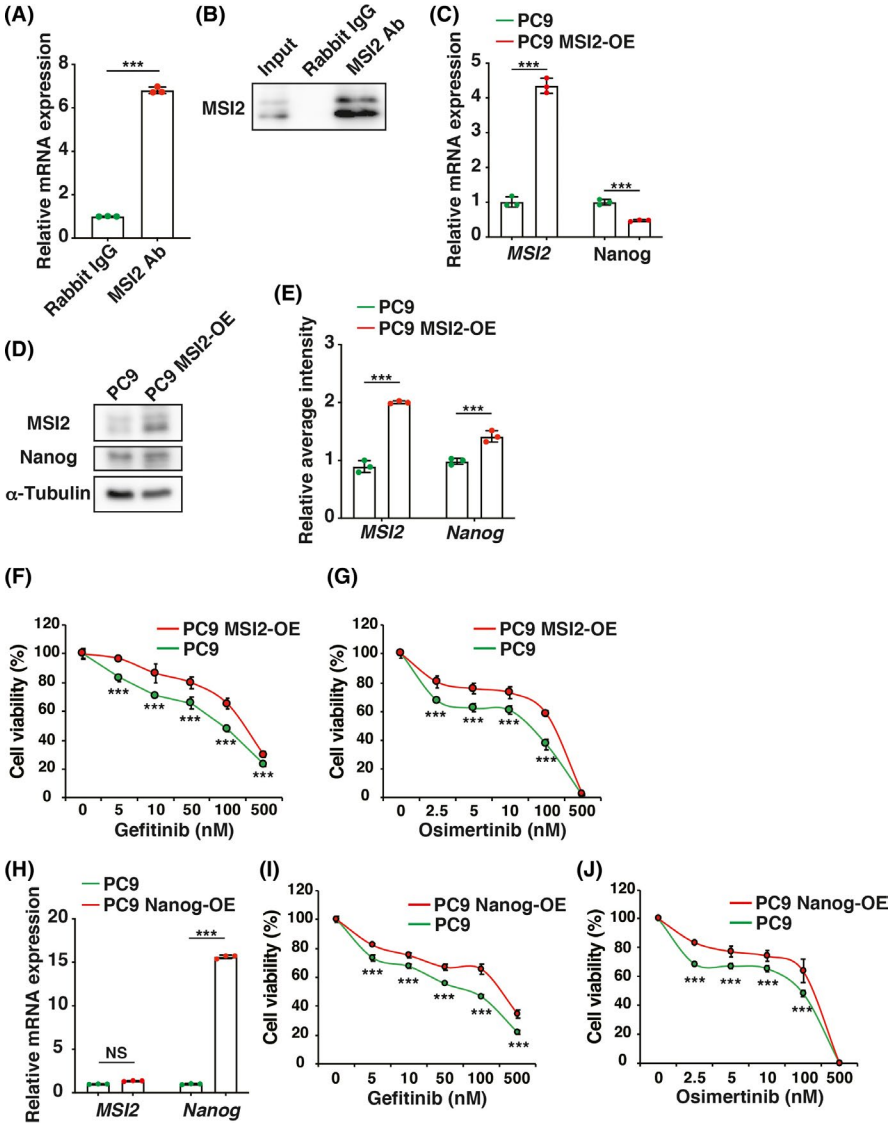

FIGURE 5 MSI2 interacts with *Nanog* mRNA and the overexpression of either MSI2 or Nanog confers resistance to gefitinib and osimertinib in PC9 cells. A, RNA immunoprecipitation (RIP) assay. RNA immunoprecipitation of MSI2 complexes with anti-MSI2 (MSI2 Ab) or control anti-rabbit IgG, followed by qPCR of *Nanog*. Relative mRNA expression of *Nanog* was enriched in anti-MSI2 antibody-coprecipitated RNA samples compared with normal rabbit IgG-coprecipitated samples. Statistical significance was determined by unpaired, two-tailed Student *t* test. Results are shown as means ± SD. n = 3 biologically independent experiments and experiments were repeated at least 3 times. B, Immunoblotting analysis as a quality check of immunoprecipitated MSI2 is shown. C, Levels of *MSI2* and *Nanog* were analyzed by qPCR in PC9 cells overexpressing MSI2 stably (PC9 MSI2-OE) or control vector-transfected cells (PC9). Results are shown as means ± SD. n = 3 biologically independent experiments and experiments were repeated at least 3 times. D, Immunoblotting analysis of MSI2 and Nanog expression in PC9 cells overexpressing MSI2 stably (PC9 MSI2-OE) or control vector-transfected cells (PC9). Representative results were shown. E, Intensities of the immunoblotting bands (D) were calculated using ImageJ software and normalized with those of α-tubulin. Statistical significance was determined by unpaired, two-tailed Student *t* test. Results are shown as means ± SD. n = 3 biologically independent experiments. F and G, PC9 cells overexpressing MSI2 stably (PC9 MSI2-OE) or control vector-transfected cells (PC9) were treated with the indicated concentrations of gefitinib (F) or osimertinib (G) for 72 h, and cell viability was measured by MTS assay. Error bars indicate SD. Non-linear regression curve was generated using MTS data. n = 3 biologically independent experiments per treatment and experiments were repeated at least 3 times. H, levels of *MSI2* and *Nanog* were analyzed by qPCR in PC9 cells overexpressing *Nanog* (PC9 Nanog-OE) or control vector-transfected cells (PC9). NS, not significant. Results are shown as means ± SEM. n = 3 biologically independent experiments and experiments were repeated at least 3 times. I and J, PC9 cells stably overexpressing Nanog (PC9 Nanog-OE) or control vector-transfected cells (PC9) were treated with the indicated concentrations of gefitinib (I) or osimertinib (J) for 72 h, and cell viability was measured by MTS assay. Error bars indicate SD. A non-linear regression curve was generated using MTS data. n = 3 biologically independent experiments per treatment and experiments were repeated at least 3 times

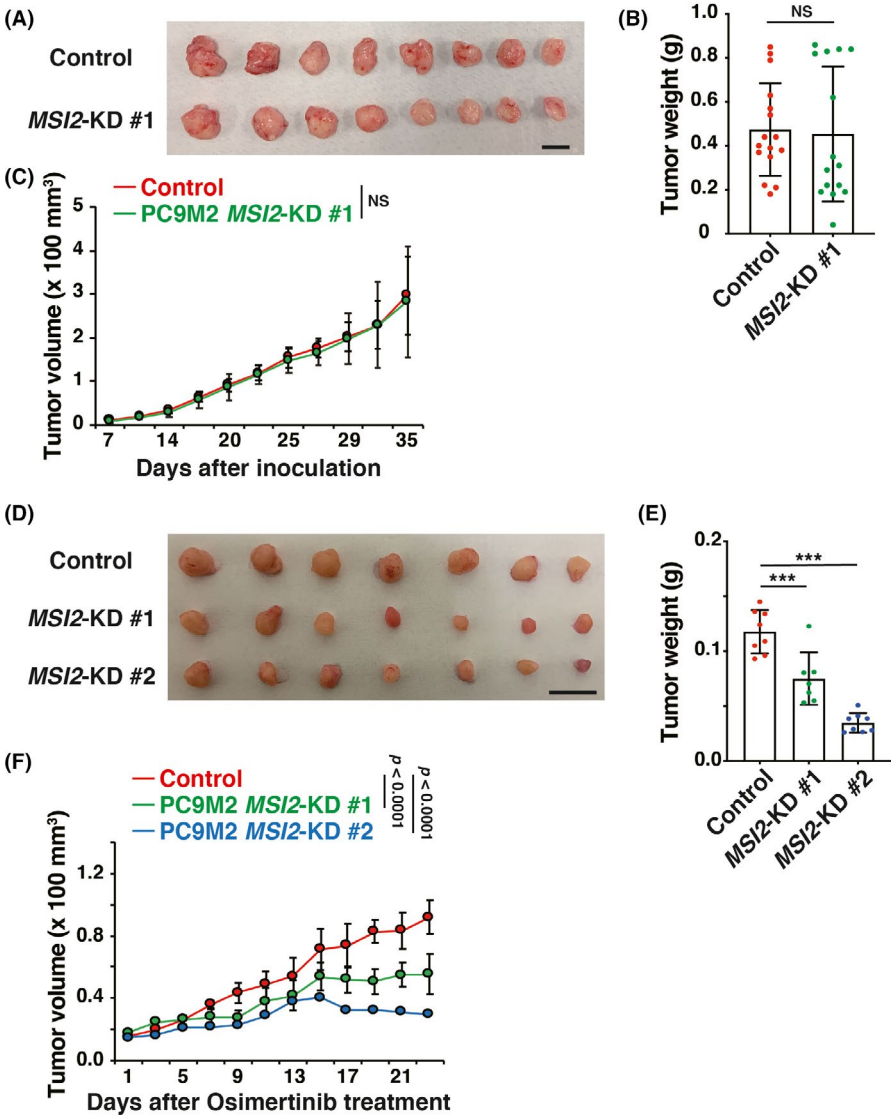

FIGURE 6 Depletion of *MSI2* restores sensitivity to osimertinib in PC9M2 cells in vivo without a significant effect on tumor growth. A-C, PC9M2 cells transduced with shRNA for MSI2 (*MSI2*-KD #1) or control vector (control) were injected into the flanks of 6-wk-old female NSG mice. NS, not significant. n = 8 mice for each condition. Macroscopic images of resected tumors at the end of the in vivo tumor growth experiment (A). Scale bar = 1 mm. Weight of the resected tumors (B). Statistical significance was determined by unpaired, two-tailed Student *t* test. Results are shown as means ± SD. In vivo tumor growth curves (C). Tumor volumes were measured. Statistical significance was determined by two-way ANOVA with Bonferroni correction. D-F, PC9M2 cells transduced with shRNAs for *MSI2* (*MSI2*-KD #1, *MSI2*-KD#2) or control vector (control) were injected into the flanks of 6-wk-old female NSG mice. n = 7 mice for each condition. Osimertinib treatment (10 mg/kg/d, 5 d/wk) was started on day 7 after inoculation and ended on day 23. Macroscopic images of resected tumors at the end of the in vivo osimertinib treatment experiment (D). Scale bar = 1 mm. Weight of resected tumors (E). Statistical significance was determined by unpaired, two-tailed Student *t* test. Results are shown as means ± SD. In vivo tumor growth curves (F). Tumor volumes were measured. Statistical significance was determined by two-way ANOVA with Bonferroni correction

without additional *EGFR* mutations. This observation suggests that MSI2 expression is a prevalent mechanism of drug resistance. To validate this possibility, it would be necessary to analyze the relationship between expression levels of MSI2 protein in NSCLC tissues and sensitivity to treatment with EGFR-TKIs in our future study. A subpopulation of NSCLC patients had increased expression levels of *MSI2* in cancer tissues and showed worse prognosis, raising the possibility that they have tolerance to EGFR-TKIs.

MSI2 binds to the 3′ untranslated region of mRNA through N-terminal RRM domains and regulates multiple functions, including protein translation and mRNA stability in a cell context-dependent manner. Several reports have shown that MSI2-binding to mRNA not only increases, but also decreases, protein translation.[23,34] Recently, genes regulated by MSI2 binding have been comprehensively analyzed in leukemia cells.[27] Although the mRNA levels of these genes were not greatly altered in association with increased MSI2 protein, the amount of protein encoded by them is significantly increased.

This is consistent with our finding that MSI2 increases Nanog at the protein level but not at the mRNA level. It can be hypothesized that MSI2 requires still undefined additional partner proteins to stabilize *Nanog* mRNA. If so, overexpression of MSI2 alone may even reduce stability of *Nanog* mRNA, as overexpression increases the amount of MSI2 proteins that do not bind to *Nanog* mRNA and may strip the partner protein from the *Nanog* mRNA.

We found that MSI2 may be involved in the increase in β-catenin protein in PC9M2 cells (data not shown). Previous studies have reported that MSI2 induced the expression of β-catenin in esophageal cancer cells,[35] whereas another report showed that MSI2 expression was not involved in β-catenin expression in colon cancer.[36] The relationship between MSI2 and β-catenin appears to be cancer type-specific.

Many efforts have been undertaken to develop specific inhibitors against RNA-binding proteins, including MSI2. Recently, a specific MSI2 inhibitor that binds to the RRM domain of MSI2 has been developed.[37] These efforts would pave the way for the development of molecularly targeted drugs specific for MSI2 and provide better treatment options for deadly cancers, including NSCLC.

ACKNOWLEDGMENTS

This work was supported in part by a research grant from Princess Takamatsu Cancer Research Fund (17-2924), a Grant-in-Aid for Scientific Research from JSPS (17K19587 and 18H02679), and a research grant from AMED Project for Development of Innovative Research on Cancer Therapeutics, Project for Cancer Research and Therapeutic Evolution (16cm0106120h0001) and Practical Research for Innovative Cancer Control (16ck0106194h0001) to NG This work was also supported by MEXT KAKENHI (No. 221S0002 and JP17H06324) to NG

DISCLOSURE

The authors declare no potential conflicts of interest.

ORCID

Takashi Kohno https://orcid.org/0000-0002-5371-706X
Noriko Gotoh https://orcid.org/0000-0003-3733-260X

REFERENCES

1. Erratum: Global cancer statistics 2018: GLOBOCAN estimates of incidence and mortality worldwide for 36 cancers in 185 countries. *CA Cancer J Clin*. 2020;70:313.
2. Testa U, Castelli G, Pelosi E. Lung cancers: molecular characterization, clonal heterogeneity and evolution, and cancer stem cells. *Cancers*. 2018;10(8):248. https://doi.org/10.3390/cancers10080248
3. Passaro A, Mok T, Peters S, Popat S, Ahn MJ, de Marinis F. Recent advances on the role of EGFR tyrosine kinase inhibitors in the management of NSCLC with uncommon, Non Exon 20 insertions, EGFR mutations. *J Thorac Oncol*. 2021;16(5):764-773. https://doi.org/10.1016/j.jtho.2020.12.002
4. Shah R, Lester JF. Tyrosine kinase inhibitors for the treatment of EGFR mutation-positive non-small-cell lung cancer: a clash of the generations. *Clin Lung Cancer*. 2020;21:e216-e228.
5. Soria JC, Ohe Y, Vansteenkiste J, et al. Osimertinib in untreated EGFR-mutated advanced non-small-cell lung cancer. *N Engl J Med*. 2018;378:113-125.
6. Wu SG, Shih JY. Management of acquired resistance to EGFR TKI-targeted therapy in advanced non-small cell lung cancer. *Mol Cancer*. 2018;17:38.
7. Tumbrink HL, Heimsoeth A, Sos ML. The next tier of EGFR resistance mutations in lung cancer. *Oncogene*. 2021;40:1-11.
8. Mehlman C, Cadranel J, Rousseau-Bussac G, et al. Resistance mechanisms to osimertinib in EGFR-mutated advanced non-small-cell lung cancer: a multicentric retrospective French study. *Lung Cancer*. 2019;137:149-156.
9. Leonetti A, Sharma S, Minari R, Perego P, Giovannetti E, Tiseo M. Resistance mechanisms to osimertinib in EGFR-mutated non-small cell lung cancer. *Br J Cancer*. 2019;121:725-737.
10. Greig SL. Osimertinib: first global approval. *Drugs*. 2016;76:263-273.
11. Alsharedi M, Bukamur H, Elhamdani A. Osimertinib for the treatment of patients with EGFR mutation-positive non-small cell lung cancer. *Drugs Today*. 2018;54:369-379.
12. Soejima K, Yasuda H, Hirano T. Osimertinib for EGFR T790M mutation-positive non-small cell lung cancer. *Expert Rev Clin Pharmacol*. 2017;10:31-38.
13. Cross DAE, Ashton SE, Ghiorghiu S, et al. AZD9291, an irreversible EGFR TKI, overcomes T790M-mediated resistance to EGFR inhibitors in lung cancer. *Cancer Discov*. 2014;4:1046-1061.
14. Mayor S. Osimertinib effective in EGFR T790M-positive lung cancer. *Lancet Oncol*. 2017;18:e9.
15. Hu X, Chen W, Li X, et al. Clinical efficacy analysis of Osimertinib treatment for a patient with leptomeningeal metastasis of EGFR+ non-small cell lung cancer without the T790M mutation. *Ann Palliat Med*. 2019;8:525-531.
16. Nagano T, Tachihara M, Nishimura Y. Mechanism of resistance to epidermal growth factor receptor-tyrosine kinase inhibitors and a potential treatment strategy. *Cells*. 2018;7(11):212.
17. Li J, Kwok HF. Current strategies for treating NSCLC: from biological mechanisms to clinical treatment. *Cancers*. 2020;12(6):1587. https://doi.org/10.3390/cancers12061587
18. Weng C-H, Chen L-Y, Lin Y-C, et al. Epithelial-mesenchymal transition (EMT) beyond EGFR mutations per se is a common mechanism for acquired resistance to EGFR TKI. *Oncogene*. 2019;38:455-468.
19. Nakata A, Yoshida R, Yamaguchi R, et al. Elevated beta-catenin pathway as a novel target for patients with resistance to EGF receptor targeting drugs. *Sci Rep*. 2015;5:13076.
20. Nakayama S, Sng N, Carretero J, et al. Beta-catenin contributes to lung tumor development induced by EGFR mutations. *Cancer Res*. 2014;74:5891-5902.
21. Zhong Z, Virshup DM. Wnt signaling and drug resistance in cancer. *Mol Pharmacol*. 2020;97:72-89.
22. Shien K, Toyooka S, Yamamoto H, et al. Acquired resistance to EGFR inhibitors is associated with a manifestation of stem cell-like properties in cancer cells. *Cancer Res*. 2013;73:3051-3061.
23. Kudinov AE, Karanicolas J, Golemis EA, Boumber Y. Musashi RNA-binding proteins as cancer drivers and novel therapeutic targets. *Clin Cancer Res*. 2017;23:2143-2153.
24. Fox RG, Lytle NK, Jaquish DV, et al. Image-based detection and targeting of therapy resistance in pancreatic adenocarcinoma. *Nature*. 2016;534:407-411.
25. Sakakibara S, Nakamura Y, Satoh H, Okano H. Rna-binding protein Musashi2: developmentally regulated expression in neural precursor cells and subpopulations of neurons in mammalian CNS. *J Neurosci*. 2001;21:8091-8107.
26. Zearfoss NR, Deveau LM, Clingman CC, et al. A conserved three-nucleotide core motif defines Musashi RNA binding specificity. *J Biol Chem*. 2014;289:35530-35541.

27. Nguyen DTT, Lu Y, Chu KL, et al. HyperTRIBE uncovers increased MUSASHI-2 RNA binding activity and differential regulation in leukemic stem cells. *Nat Commun*. 2020;11:2026.
28. Nishimura T, Nakata A, Chen X, et al. Cancer stem-like properties and gefitinib resistance are dependent on purine synthetic metabolism mediated by the mitochondrial enzyme MTHFD2. *Oncogene*. 2019;38:2464-2481.
29. Tominaga K, Minato H, Murayama T, et al. Semaphorin signaling via MICAL3 induces symmetric cell division to expand breast cancer stem-like cells. *Proc Natl Acad Sci USA*. 2019;116:625-630.
30. Hu Y, Smyth GK. ELDA: extreme limiting dilution analysis for comparing depleted and enriched populations in stem cell and other assays. *J Immunol Methods*. 2009;347:70-78.
31. Reya T, Clevers H. Wnt signalling in stem cells and cancer. *Nature*. 2005;434:843-850.
32. Wang S, Li N, Yousefi M, et al. Transformation of the intestinal epithelium by the MSI2 RNA-binding protein. *Nat Commun*. 2015;6:6517.
33. Bennett CG, Riemondy K, Chapnick DA, et al. Genome-wide analysis of Musashi-2 targets reveals novel functions in governing epithelial cell migration. *Nucleic Acids Res*. 2016;44:3788-3800.
34. Kudinov AE, Deneka A, Nikonova AS, et al. Musashi-2 (MSI2) supports TGF-beta signaling and inhibits claudins to promote non-small cell lung cancer (NSCLC) metastasis. *Proc Natl Acad Sci USA*. 2016;113:6955-6960.
35. Li Z, Jin H, Mao G, Wu L, Guo Q. Msi2 plays a carcinogenic role in esophageal squamous cell carcinoma via regulation of the Wnt/beta-catenin and Hedgehog signaling pathways. *Exp Cell Res*. 2017;361:170-177.
36. Li N, Yousefi M, Nakauka-Ddamba A, et al. The Msi family of RNA-binding proteins function redundantly as intestinal oncoproteins. *Cell Rep*. 2015;13:2440-2455.
37. Minuesa G, Albanese SK, Xie W, et al. Small-molecule targeting of MUSASHI RNA-binding activity in acute myeloid leukemia. *Nat Commun*. 2019;10:2691.

SUPPORTING INFORMATION

Additional supporting information may be found online in the Supporting Information section.

How to cite this article: Yiming R, Takeuchi Y, Nishimura T, et al. MUSASHI-2 confers resistance to third-generation EGFR-tyrosine kinase inhibitor osimertinib in lung adenocarcinoma. *Cancer Sci*. 2021;112:3810–3821. https://doi.org/10.1111/cas.15036